

## Magnetic-field-induced insulator-quantum Hall-insulator transition in a disordered two-dimensional electron gas

This article has been downloaded from IOPscience. Please scroll down to see the full text article.

1994 J. Phys.: Condens. Matter 6 4763

(<http://iopscience.iop.org/0953-8984/6/25/014>)

View [the table of contents for this issue](#), or go to the [journal homepage](#) for more

Download details:

IP Address: 171.66.16.147

The article was downloaded on 12/05/2010 at 18:42

Please note that [terms and conditions apply](#).

## Magnetic-field-induced insulator–quantum Hall–insulator transition in a disordered two-dimensional electron gas

R J F Hughes†, J T Nicholls†, J E F Frost†, E H Linfield†, M Pepper†, C J B Ford†, D A Ritchie†, G A C Jones†, Eugene Kogan‡† and Moshe Kaveh‡†

† Cavendish Laboratory, Madingley Road, Cambridge CB3 0HE, UK

‡ The Jack and Pearl Resnick Institute of Advanced Technology, Department of Physics, Bar-Ilan University, Ramat-Gan 52900, Israel

Received 19 January 1994, in final form 31 March 1994

**Abstract.** We present low-temperature transport measurements on the two-dimensional electron gas in  $\delta$ -doped GaAs which undergoes an insulator–quantum Hall–insulator transition as the magnetic field is increased. Both low- and high-field transitions are marked by peaks in  $\sigma_{xx}$  and the temperature-independent critical value of  $\sigma_{xy}$  of  $0.5e^2/h$  per spin. We map out the phase diagram versus disorder and magnetic field and study the temperature dependence of  $\sigma_{xx}$  throughout. In the quantum Hall region we observe Mott variable range hopping and, around the high-field transitions, scaling via a single parameter:  $z = (B - B^*)T^{-0.45}$ . The functional dependence on  $z$  above this transition is fitted by recent network percolation calculations.

The transport properties of a two-dimensional electron gas (2DEG) continue to attract much interest both experimentally and theoretically. In particular, the simultaneous presence of both disorder and a strong magnetic field leads to a rich variety of phenomena of which probably the most vivid is the quantum Hall effect [1].

The theoretical phase diagram [2, 3] for the integral quantum Hall effect, showing the stable  $T = 0$  phases as a function of disorder and perpendicular magnetic field  $B$ , is shown in figure 1(a). Starting from the insulator at  $B = 0$  with some fixed level of disorder, it is possible to observe a sequence of transitions from insulator through various quantum Hall liquids and then back to the insulator by increasing the perpendicular magnetic field. In the simplest picture of the quantum Hall effect, each transition, characterized by a peak in  $\sigma_{xx}$  and a step in  $\sigma_{xy}$ , is a consequence of the extended states at a Landau level centre passing through the Fermi energy. The quantum Hall index  $s_{xy}$ , which counts the number of energies below the Fermi level at which extended states exist, decreases by one at each transition until the insulator ( $s_{xy} = 0$ ) is reached. However, since all states are localized at zero magnetic field, a series of ‘delocalization’ transitions is required at low fields in which extended levels pass *downwards* through the Fermi energy and  $s_{xy}$  is incremented. The first theory [2] for this sequence of transitions, based on two-parameter scaling [4], proposed a simple interpolation formula to describe how extended states shift in energy with magnetic field. In this model, as the magnetic field rises, extended states sink in energy and cross the Fermi level until the point is reached where disorder-broadened Landau levels become well resolved. As the magnetic field is further increased, the extended states sit at Landau level centres and rise in energy, eventually recrossing the Fermi level. More recently this phase

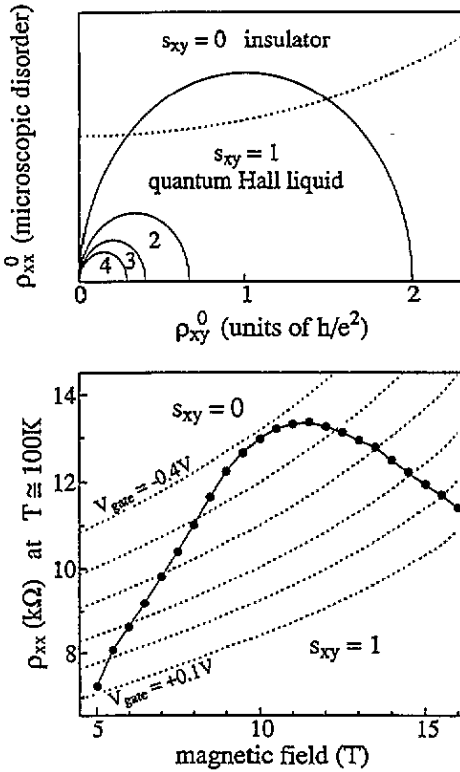


Figure 1. (a) Theoretical phase diagram [3] (microscopic disorder versus classical Hall resistance  $\rho_{xy}^0 \propto B$ ) for the integral quantum Hall effect. The dotted line shows schematically the path followed in our experiment. (b) Experimental phase diagram showing the top section of the  $s_{xy} = 1 \leftrightarrow 0$  phase boundary. The dotted construction lines are the device magnetoresistivities at  $T \sim 100$  K in gate voltage steps of 0.1 V.

diagram has been reproduced and extended by a global theory [3] which is also applicable to the fractional quantum Hall effect.

Experimentally, no low-field transitions were observed until recently [5] since in high-mobility devices the states are only weakly localized at low magnetic fields and transport is diffusive. Support for the global phase diagram [3] does exist in the fractional regime [6, 7] while evidence inconsistent with it has been obtained from low density silicon devices [8]. The first part of this paper reports measurements on low-mobility devices which enable us to map the  $s_{xy} = 1 \leftrightarrow 0$  phase boundary in detail and examine the critical behaviour of the conductivity at the transition.

In the second part we examine the finite-temperature properties of such a 2DEG where most previous experiments have concentrated on the conductivity only at Shubnikov-de Haas (SdH) minima. Here various authors have found simple activation [9], Coulomb-gap-induced  $T^{1/2}$  variable-range hopping (VRH) [10, 12] or Mott's  $T^{1/3}$  VRH [11, 5]. In the critical region it is not clear whether the conductivity should show activated [12] or quasi-metallic [13, 14] behaviour. Our study of the temperature dependence of the conductivity over a wide range of magnetic fields answers some of these questions. We find that in the quantum Hall phase, everywhere except for the critical regions, the conductivity fits Mott's VRH formula. Around the upper critical magnetic field we find that  $\sigma_{xx}(B, T)$  obeys a one-parameter scaling law which agrees with calculations [15] based on a quantum percolation network model.

We now discuss in detail our experimental set-up and results. The devices used in this study were fabricated from MBE-grown  $\delta$ -doped GaAs wafers. An n-type Si-doped plane was incorporated into a 0.55  $\mu\text{m}$  thick undoped GaAs film to form a deep potential well in which

the 2DEG is confined close to the ionized donors and is therefore highly disordered. Three different wafers have shown similar behaviour but the detailed measurements described below were carried out on just one wafer for which the carrier density was  $4 \times 10^{11} \text{ cm}^{-2}$  in a layer  $0.3 \mu\text{m}$  below the surface. Wet etching was used to define rectangular Hall bars of width  $80 \mu\text{m}$  with voltage probes spaced  $640 \mu\text{m}$  apart. Control over the carrier concentration, and thereby also the screening and effective disorder, was provided by application of a voltage to a surface nichrome-gold Schottky gate. Transport measurements were carried out at temperatures between 50 mK and 1 K in a dilution refrigerator using standard *ac* lock-in techniques. The four-terminal longitudinal and Hall resistivities  $\rho_{xx}$  and  $\rho_{xy}$  were measured simultaneously using an excitation voltage of  $10 \mu\text{V}$  or less at a frequency of 14.5 Hz. By comparing measurements on samples with different aspect ratios, we have checked that the resistivity (not the resistance) is the critical quantity close to the transitions.

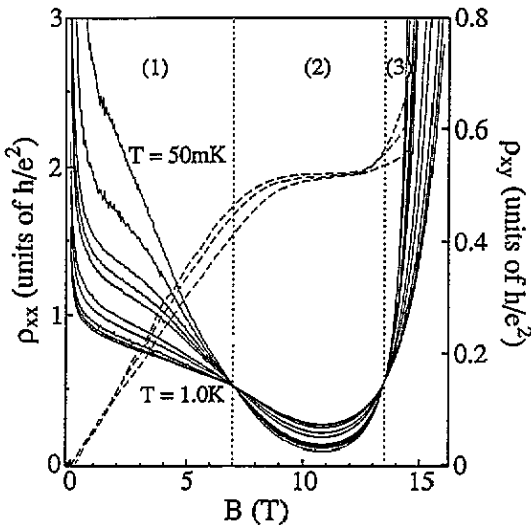


Figure 2. Solid curves:  $\sigma_{xx}$  at  $T = 50, 90, 175, 215, 250, 445, 580, 795, 915$  and  $1020 \text{ mK}$  and  $V_{\text{gate}} = -0.2 \text{ V}$ . Dashed curves:  $\rho_{xy}$  at  $T = 50, 445$  and  $1020 \text{ mK}$ . Vertical dotted lines mark the critical magnetic fields  $B_{(1)}^*$  and  $B_{(2)}^*$  separating the quantum Hall region (2) from the insulating regions (1) and (3).

When the magnetic field is swept at a set of different temperatures,  $\rho_{xx}$  exhibits two temperature-independent crossing points, similar to the results of Jiang *et al* [5], between which  $\rho_{xy}$  is close to its plateau value (figure 2). Figure 3 shows the conductivity components  $\sigma_{xx}$  and  $\sigma_{xy}$ , obtained by inverting the resistivity tensor, at a gate voltage of  $-0.2 \text{ V}$ . Two clear transitions are observed where the temperature dependences of  $\sigma_{xy}$  (and  $\rho_{xx}$ ) change sign at critical magnetic fields  $B_{(1)}^*$  and  $B_{(2)}^*$  and the curves cross at a point. The regions labelled (1) and (3) are insulating, with  $\sigma_{xx} \rightarrow 0$  and  $\sigma_{xy} \rightarrow 0$  as  $T \rightarrow 0$ . Region (2) is the filling factor two quantum Hall state, with  $\sigma_{xx} \rightarrow 0$  and  $\sigma_{xy} \rightarrow 2e^2/h$  as  $T \rightarrow 0$ , corresponding to a partially filled lowest Landau level with spin degeneracy two. The Landau level is not strictly degenerate in the sense  $g\mu_B B < kT$  but we cannot resolve the spin splitting because it is much smaller than the disorder broadening. The extra peak predicted [2] for  $\sigma_{xx}$  is at  $7.0 \text{ T}$  and coincides with an *upward* step to a plateau in  $\sigma_{xy}$ .

Although our data, like those of Jiang *et al* [5], display quite sharp crossing points in  $\rho_{xx}$ , we believe that  $\sigma_{xy}$ , which also shows temperature-independent points, is the more important quantity. In the scaling theory of the quantum Hall effect [4], values of  $\sigma_{xy}$  that are half integral multiples of  $e^2/h$  (per spin) behave as fixed points under renormalization. This is an assumption in the theory of Khmel'nitskii [2] which our experiment clearly

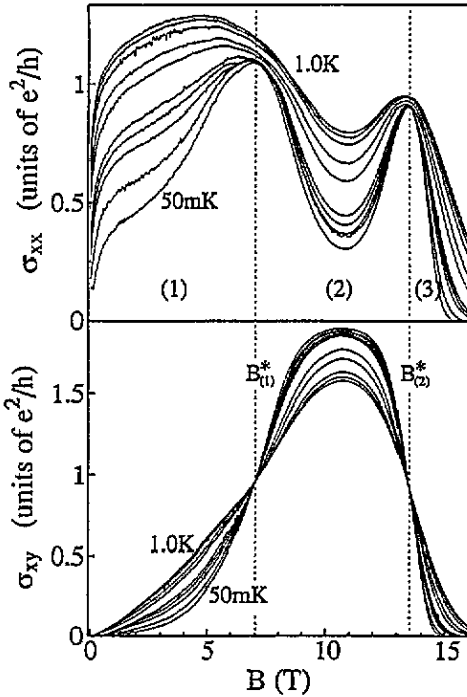


Figure 3.  $\sigma_{xx}$  and  $\sigma_{xy}$  calculated from the data of figure 2 by matrix inversion.

corroborates at both transitions. In the same temperature range, on the other hand,  $\sigma_{xx}$  is weakly temperature dependent at the transitions with magnitude approximately equal to  $e^2/h$ . Given the good agreement between theoretical expectations and the experimental values of the conductivity components at the transitions, it is reasonable to explain the virtual temperature independence of  $\rho_{xx}$  as coincidence specific to the transition between filling factors zero and two. This follows from matrix inversion assuming  $\sigma_{xy} \simeq \sigma_{xx}$  with  $\sigma_{xx}$  varying only weakly. Although our data do not show this, we would not necessarily expect temperature-independent behaviour for  $\rho_{xx}$  at transitions between other filling factors where  $\sigma_{xy} \neq \sigma_{xx} \simeq e^2/h$ .

Curves like those in figures 2 and 3 correspond to a slice through the phase diagram along something like the trajectory shown as a dotted line in figure 1(a). Repeating the measurement for different levels of disorder by adjusting the gate voltage, we can shift the critical magnetic fields and so map out an experimental phase diagram. As the gate voltage is made increasingly negative, the width of the quantum Hall region diminishes until at  $-0.385$  V it just vanishes. There is still a pronounced minimum in  $\rho_{xx}(B)$  and a weak plateau in  $\rho_{xy}(B)$  at more negative gate voltages, where the device is always insulating, presumably due to critical quantum-Hall-like fluctuations that persist into the insulating phase.

Our experimental phase diagram is plotted in figure 1(b). In reality the disorder cannot be expected to remain constant with magnetic field: wavefunction shrinkage will increase the effective disorder at high magnetic fields, hence the upward curve to the dotted trajectory in figure 1(a). This variation we determined empirically from the device magnetoresistivity measured at a high temperature and used to calibrate the disorder axis in figure 1(b) (dotted construction lines). The theories [2, 3] parametrize disorder via a Drude-type conductivity on a microscopic length scale of the order of the magnetic length and the nearest experimental

analogue is the high-temperature (classical) resistance which is determined on the scale of the inelastic length. The aim is to make our phase diagram as independent as possible of sample-dependent microscopic details although we have neglected the small (15%) change in carrier concentration which occurs in our experiment. The high temperature we have used,  $T \sim 100$  K, may introduce complications in that new mechanisms could affect the transport but, in any case, our measure of disorder increases monotonically with negative gate voltage and with magnetic field and therefore cannot alter the topology of the  $\sigma_{xy} = 1 \leftrightarrow 0$  boundary which is seen to be as theoretically predicted [2, 3].

Turning now to the finite-temperature behaviour of  $\sigma_{xx}$ , throughout the entire magnetic field range our data, within the experimental error, fits the 2D Mott hopping formula:  $\sigma_{xx} = \sigma_0 \exp -(T_0/T)^{1/3}$  where  $\sigma_0$  is assumed constant and  $T_0 \propto 1/\xi^2$ ,  $\xi$  being the localization length. The range over which  $\sigma_{xx}$  varies is too small (an order of magnitude or less) to clearly distinguish between the Mott law and the Efros–Shklovskii law, which has exponent  $\frac{1}{2}$ . However, in the quantum Hall regions at low disorders, where  $\sigma_{xx}$  varies most, several pieces of evidence combine to favour the Mott formula. Firstly, in this region we can fit the data allowing the power in the hopping formula to vary freely as well as  $\sigma_0$  (assumed temperature independent) and  $T_0$ , and find it to be  $0.32 \pm 0.02$ . The error describes the scatter in fits taken at different magnetic fields throughout the central 70% of the quantum Hall region where the  $\sigma_{xx}$  variation is sufficiently great. One might expect this value to be affected by any possible temperature dependence of the prefactor  $\sigma_0$  but the independence of the exponent on magnetic field is reassuring. The value obtained for  $\sigma_0$  also remains fairly constant at a reasonable value of about  $e^2/h$ . The  $T^{1/3}$  law fit also gives the correct localization length exponent near the transition: according to theory and experiment [16],  $\xi$  diverges as  $\xi \sim |B - B^*|^{-\nu}$  near the centre of a disorder-broadened Landau level with  $\nu \simeq 2.3$ . From fits assuming the  $T^{1/3}$  law we find near the transitions but not so close that hopping breaks down, that  $T_0 \sim |B - B^*|^x$  with  $x = 5 \pm 1$ . This agrees with  $T_0 \propto 1/\xi^2$  in the Mott equation which implies  $x = 2\nu = 4.7$ . If we carry out the same procedure for fits assuming the  $T^{1/2}$  law we obtain approximately the same experimental value for  $x$  but, since the Efros–Shklovskii law has  $T_0 \propto 1/\xi$ , the theoretical expectation would be  $x = \nu = 2.3$ . Finally, the  $T^{1/2}$  law fitted to our data gives unphysical localization lengths, greater than the sample size. Mott  $T^{1/3}$  hopping is rarely observed in measurements taken at  $\rho_{xx}$  minima; a Coulomb-gap-induced  $T^{1/2}$  dependence is more common. However, our fits yield hopping lengths which are unusually large, greater than the separation between gate metal and 2DEG. The explanation for  $T^{1/3}$  behaviour may therefore be that the gate is effective at screening the hopping charges and the Coulomb gap in the density of states is removed.

Next we consider the conductivity in the critical region around  $B_{(2)}^*$ , where the temperature dependence is too weak to distinguish between alternative possible forms for  $\sigma_{xx}(T)$ . Here it is predicted [13] that the transport is quasi-metallic once the localization length is greater than the inelastic length and can be described as a function of a single parameter,  $z = (B - B^*)T^{-\mu}$ , where  $\mu$  is a critical exponent. Our experimental  $\sigma_{xy}$  curves do indeed collapse onto universal functions of  $z$  for  $\mu = 0.45 \pm 0.05$  while for  $\sigma_{xx}$ , due to a slight temperature dependence even at the transition, the scaling is worse (figure 4 inset). Previous experiments [17–19], focusing on the half-width of the  $\rho_{xx}$  peak and the derivatives of the Hall resistivity,  $d^{(n)}\rho_{xy}/dB^{(n)}$ , half-way between plateaux, have obtained a range of values for  $\mu$ . Our result is consistent with the value  $\mu = 0.43 = 3/7$  [17] explained by various theories [13, 14, 20].

For  $B > B_{(2)}^*$ , the scaling of  $\sigma_{xx}$  is good over the whole height of the peak and, moreover, is quantitatively well described by the scaling function [15] calculated for a

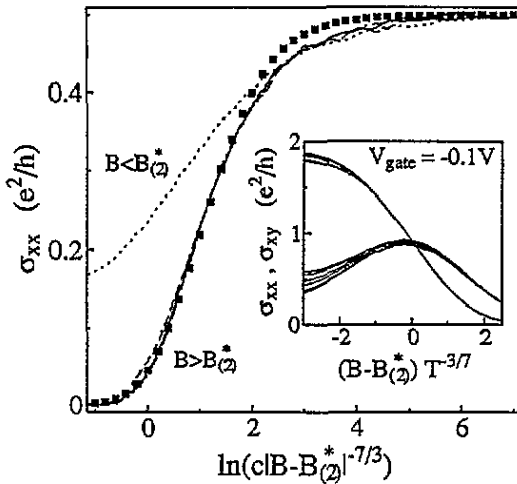


Figure 4. Best fits to the scaling results [15] (squares) for  $\sigma_{xx}(B)$  at  $T = 50$  mK. The three coinciding curves are for  $B > B_{(2)}^*$  at  $V_{gate} = -0.2$  V (solid),  $-0.1$  V (dashed) and  $0.0$  V (dot-dashed) after scaling  $\sigma_{xx(max)}$  to  $0.5e^2/h$ . The dotted curve is for  $B < B_{(2)}^*$  at  $-0.2$  V. Inset: the conductivity versus  $(B - B_{(2)}^*)T^{-0.43}$  around  $B_{(2)}^* = 14.6$  T at  $V_{gate} = -0.1$  V for seven temperatures between 0.2 K and 1 K.

network quantum percolation model. This is shown in figure 4 where our experimental  $\sigma_{xx}$  has been scaled down by a factor of just over two so that its height is exactly  $0.5e^2/h$  and then fitted to the numerical results [15], assuming  $\mu = 3/7$ , via a single parameter  $c$  which determines the horizontal position of the curve. The same calculations were also successfully fitted [15] to data for the  $s_{xy} = 3 \leftrightarrow 2$  transition indicating that both quantum Hall–quantum Hall and quantum Hall–insulator transitions are in the same universality class [21].

For  $B < B_{(2)}^*$ , the scaling is worse, perhaps because of the overlap between the peaks, and the calculations do not fit the data. The approximate scaling function obtained can be fitted to a simple activation law for  $\sigma_{xx} > 0.7e^2/h$  while for  $\sigma_{xx} < 0.6e^2/h$  our VRH fit is good, yielding a best exponent of close to 0.33. This lends credence to the VRH approach to the temperature dependence of the peak width adopted in [12] but the prediction  $\mu = 0.42$  requires Efros–Shklovskii rather than Mott VRH. On the other hand, the value  $\mu = 0.42$  from scaling arguments is independent of the precise functional dependence of  $\sigma_{xx}$  on  $z$ .

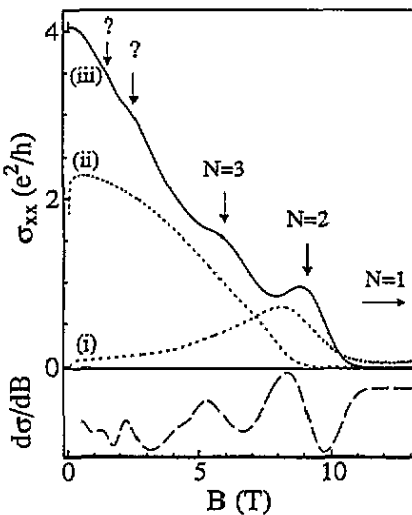


Figure 5. Conductance versus magnetic field for a Corbino device at full illumination (iii) and at two intermediate stages (i) and (ii). The weak features (?) at low fields are accentuated in a numerical derivative (lower graph) of curve (iii).

Finally, it is interesting to see whether more of the left-hand side of the phase diagram can be observed, for example the  $s_{xy} = 1 \leftrightarrow 2$  transition. One problem is that, as the disorder is reduced, a sample of practicable size may become weakly localized at  $B = 0$  before the  $s_{xy} = 2$  phase is reached. To check whether this is the case we used ungated Corbino devices made from the same material and reduced the disorder via progressive illumination utilizing the persistent photoconductivity effect. Results on discs of inner and outer radii of 480 and 760  $\mu\text{m}$ , respectively, show metallic behaviour at  $B = 0$  before the  $N = 2$  SdH oscillation is visible. Surprisingly, however, close to full illumination, even though  $\sigma_{xx}(0) \gg e^2/h$ , there are very weak features in  $\sigma_{xx}(B)$  at 50 mK (figure 5, curve (iii)) which might correspond to delocalization transitions. The first three SdH peaks are seen at  $B = 18, 9$  and  $6$  T but the fourth is not visible at  $4.5$  T. Two extra features (enhanced in the figure via a numerical derivative) occur at lower fields of  $1.5$  and  $2.5$  T. Since  $\sigma_{xy}$  cannot be measured on these devices, we cannot use the quantization of the Hall conductivity to identify these as phase transitions, nor do we have a great enough experimental range to verify that these peaks shift in the opposite direction to the SdH peaks as the disorder is varied. What we do observe after successive illuminations (curves (i) and (ii)) is that the  $\sigma_{xy} = 0 \leftrightarrow 1$  peak shifts to lower fields and is lost in the metallic background before the  $N = 2$  SdH peak appears. The  $N = 3$  SdH oscillation emerges next at about the same stage as the two weak low-field features. If we speculate that the new features do mark quantum Hall delocalization transitions, then the associated divergences of localization length will not much affect transport in the weakly localized regime, and transitions other than  $s_{xy} = 0 \leftrightarrow 1$  will be very difficult to observe clearly.

In conclusion we have observed an insulator–quantum Hall–insulator transition by applying a perpendicular magnetic field to a highly disordered 2DEG and have mapped out part of the phase diagram using a Schottky gate to vary the disorder. In the quantum Hall liquid state, apart from the critical regions, we have found Mott VRH. The localization length diverges as the transitions are approached and here we observe single-parameter scaling:  $\sigma_{\alpha\beta} = \sigma_{\alpha\beta}(B - B^*)T^{-\mu}$ , where  $\mu \simeq 3/7$ . The form of  $\sigma_{xx}(B, T)$  above the high-field transition is well described by recent calculations.

## Acknowledgments

This work was supported by the Science and Engineering Research Council. We thank D E Khmel'nitskii, B I Shklovskii and Y Avishai for useful discussions and especially S Kivelson and Z Wang who provided us with the results of their numerical calculations. MK and EK acknowledge the warm hospitality of the Semiconductor Physics group at the Cavendish Laboratory where this work was carried out, and also the support of the Israeli Academy of Sciences. JTN acknowledges support from the Isaac Newton Trust. Since this work was carried out, similar experiments have also been performed by Friedland *et al* [22] and Wang *et al* [23].

## References

- [1] Prange R E and Girvin S M 1987 *The Quantum Hall Effect* (Berlin: Springer)
- [2] Khmel'nitskii D E 1984 *Phys. Lett.* **106A** 182
- [3] Kivelson S, Lee D-H and Zhang S-C 1992 *Phys. Rev. B* **46** 2223
- [4] Pruisken A M M in [1]
- [5] Jiang H W *et al* 1993 *Phys. Rev. Lett.* **71** 1439



- [6] Jiang H W et al 1991 *Phys. Rev. B* **44** 8107
- [7] Sajoto T et al 1993 *Phys. Rev. Lett.* **70** 2321
- [8] D'Iorio M, Pudalov V M and Semenchinsky S G 1990 *Phys. Lett.* **150A** 422
- [9] Pepper M 1978 *Phil. Mag.* **B 37** 83
- [10] Briggs A et al 1983 *Phys. Rev. B* **27** 6549
- [11] Störmer H L, Tsui D C and Gossard A C 1982 *Phys. Rev. B* **25** 1405
- [12] Polyakov D G and Shklovskii B I 1993 *Phys. Rev. Lett.* **70** 3796
- [13] Pruisken A M M 1988 *Phys. Rev. Lett.* **61** 1297
- [14] Zhao H L and Feng S 1993 *Phys. Rev. Lett.* **70** 4134
- [15] Lee D H, Wang Z and Kivelson S 1993 *Phys. Rev. Lett.* **70** 4130
- [16] Koch S, Haug R J, von Klitzing K and Ploog K 1992 *Phys. Rev. B* **46** 1596
- [17] Wei H P, Tsui D C, Paalanen M A and Pruisken A M M 1988 *Phys. Rev. Lett.* **61** 1294  
Engel L et al 1990 *Surf. Sci.* **229** 13
- [18] Koch S, Haug R J, von Klitzing K and Ploog K, 1991 *Phys. Rev. B* **43** 6828
- [19] Dolgoplov V T et al 1991 *Zh. Eksp. Teor. Fiz.* **99** 201 (Engl. Transl. *Sov. Phys.-JETP* **72** 113)
- [20] Sondhi S L and Kivelson S A 1993 unpublished
- [21] Kivelson S 1993 private communication
- [22] Friedland K-J, Hey R, Koch S and Rentzsch R 1993 *Proc. 5th Int. Conf. on Hopping and Related Phenomena (Glasgow)*
- [23] Wang T, Clark K P, Spencer G F, Mack A M and Kirk W P 1994 *Phys. Rev. Lett.* **72** 709